Preliminary Analysis of Pressure Gradient for Two-Phase Flow and Dryout Heat Flux through Beds composed of Debris resulted from TROI Tests

Jin Ho Park [a*], Sang Mo An [a*], Jaehoon Jung [a], Seong-Wan Hong [a]
[a]*Thermal Hydraulics and Severe Accident Division, Korea Atomic Energy Research Institute, 989-111 Daedeok-daero, Yuseong-gu, Daejeon 34057, Korea*
[*]*Corresponding author: sangmoan@kaeri.re.kr*

1. Introduction

When severe accident occurs and progresses to the ex-vessel phase by reactor pressure vessel failure in light water reactors, the molten core material (corium) is relocated into the water-filled reactor cavity as a severe accident management measure. The assurance of the ex-vessel debris bed coolability is crucial since it is the pre-conditions of molten corium concrete interaction resulting in concrete floor erosion which threaten to the integrity of nuclear power plant containment. Therefore, to terminate severe accident progression ultimately, it is essential to supply sufficient coolant into the internally heat generating debris bed on the cavity floor. Because effectiveness of such coolant ingression into a debris bed is determined by the pressure gradient through porous debris bed, it is significant to investigate the pressure drop mechanisms and resulting coolability in the debris bed characterized by geometric parameters (porosity, diameter, morphology, size distribution of particles etc.).

Thus, through the numerous researchers [1-8], various two-phase flow models were suggested based on the results of dryout heat flux and isothermal air/water flow experiments through porous media composed of mono-sized spherical particles. In regard to effects of particle morphology and/or the particle size distribution on the pressure gradients in particle beds, various modified Ergun constants (C_1 and C_2) and mean diameters (d_{sd} and d_{eq} for non-spherical particle, d_m, d_a, d_l and d_n for particle size distribution) were suggested and it was well organized in the studies [9, 10].

Nevertheless, there still exists uncertainty on irregular shaped particles with size distribution for the safety analysis of ex-vessel debris bed coolability. Therefore, the preliminary analysis is performed to investigate the uncertainty of pressure drop and dryout heat flux predicted by the existing two-phase flow models in beds composed of particles from TROI tests [11] before conducting the experiments. TROI tests are to investigate the prototypic corium-water interaction. Thus, the evaluation of coolability using debris characteristics resulted from TROI tests is extremely meaningful.

2. Models

2.1 Pressure Drop for Two-Phase Flow

The pressure drop models for two-phase flow in porous media are expressed by Eqs. (1) and (2) for liquid and gas, respectively:

$$-\frac{dp_l}{dz} = \rho_l g + \frac{\mu_l}{KK_{rl}} V_{sl} + \frac{\rho_l}{\eta\eta_{rl}} V_{sl}\left|V_{sl}\right| - \frac{F_i}{s}, \quad (1)$$

$$-\frac{dp_g}{dz} = \rho_g g + \frac{\mu_g}{KK_{rg}} V_{sg} + \frac{\rho_g}{\eta\eta_{rg}} V_{sg}\left|V_{sg}\right| + \frac{F_i}{\alpha}, \quad (2)$$

where $-dp/dz$ represents pressure gradient in porous media, V_{si} (i: phase; l = liquid, g = gas) is superficial velocity of fluid. ρ_i and μ_i are the dynamic density and the viscosity of fluid. K_{rl}, K_{rg} and η_{rl}, η_{rg} are the relative permeabilities and passabilities of liquid and gas. F_i is the interfacial drag between liquid and gas and s (=$1-\alpha$) is the liquid saturation. K and η, Eq. (3) are the permeability and the passability, respectively,

$$K = \frac{\varepsilon^3 d_p^2}{C_1(1-\varepsilon)^2}, \ \eta = \frac{\varepsilon^3 d_p}{C_2(1-\varepsilon)}, \quad (3)$$

where C_1 and C_2 are the empirical Ergun constants, d_p and ε are the particle diameter and the bed porosity, Eq. (4) which is obtained by the mass of particles m_p in a test section, the density of particles ρ_p, and the volume of the test section V_t.

$$\varepsilon = 1 - \frac{\sum(m_p / \rho_p)}{V_t} \quad (4)$$

Among various models, the formulas of a model proposed by Park et al. [8] are listed in Tables I and II, representatively and a detailed description on the other models can be found in their studies [1-7].

Table I: Relative permeabilities, passabilities according to flow regime for the model proposed by Park et al. [8]

	Flow regime	K_{rg}	η_{rg}	K_{rl}	η_{rl}
$0 < \alpha < \alpha_1$	Bubbly	$\left(\frac{1-\varepsilon}{1-\varepsilon\alpha}\right)^{4/3}\alpha^4$	$\left(\frac{1-\varepsilon}{1-\varepsilon\alpha}\right)^{2/3}\alpha^4$	s^3	s^5
$\alpha_1 < \alpha < \alpha_2$	From bubbly to slug				
$\alpha_2 < \alpha < \alpha_3$	Slug				
$\alpha_3 < \alpha < \alpha_4$	From slug to annular	$\frac{\left(\frac{1-\varepsilon}{1-\varepsilon\alpha}\right)^{4/3}\alpha^3}{\left(W+\frac{1-W}{\alpha}\right)}$	$\frac{\left(\frac{1-\varepsilon}{1-\varepsilon\alpha}\right)^{2/3}\alpha^3}{\left(W+\frac{1-W}{\alpha}\right)}$		
$\alpha > \alpha_4$	Annular	$\left(\frac{1-\varepsilon}{1-\varepsilon\alpha}\right)^{4/3}\alpha^3$	$\left(\frac{1-\varepsilon}{1-\varepsilon\alpha}\right)^{2/3}\alpha^3$		

Table II: Interfacial drag according to flow regime for model proposed by Park et al. [8]

	F_i
$0<\alpha<\alpha_1$	$C_{v,B}=18(\alpha_0 f+\alpha-\alpha_0)$ $C_{i,B}=0.34s^3(\alpha_0 f^2+\alpha-\alpha_0)$ $F_{i,B}=C_{v,B}\frac{\mu_l}{D_b^2\varepsilon}sV_r+C_{i,B}\frac{(s\rho_l+\alpha\rho_g)}{D_b\varepsilon^2}s^2V_r\lvert V_r\rvert$
$\alpha_1<\alpha<\alpha_2$	$C_{v,BS}=C_{v,BH}(1-W)+C_{v,S}W$ $C_{i,BS}=C_{i,BH}(1-W)+C_{i,S}W$ $F_{i,BS}=C_{v,BS}\frac{\mu_l}{D_b^2\varepsilon}sV_r+C_{i,BS}\frac{(s\rho_l+\alpha\rho_g)}{D_b\varepsilon^2}s^2V_r\lvert V_r\rvert$
$\alpha_2<\alpha<\alpha_3$	$C_{v,S}=5.21\alpha,\ C_{i,S}=0.92s^3\alpha$ $F_{i,S}=C_{v,S}\frac{\mu_l}{D_b^2\varepsilon}sV_r+C_{i,S}\frac{(s\rho_l+\alpha\rho_g)}{D_b\varepsilon^2}s^2V_r\lvert V_r\rvert$
$\alpha_3<\alpha<\alpha_4$	$F_{i,SA}=F_{i,S}(1-W)+F_{i,A}W$
$\alpha>\alpha_4$	$F_{i,A}=\left(\frac{\mu_g}{KK_{rg}}s\alpha V_r+\frac{\rho_g}{\eta\eta_{rg}}s\alpha^2V_r\lvert V_r\rvert\right)\times(1-\alpha)^4\min\left(1,\left(\frac{d_p}{6\,mm}\right)^2\right)$

The void fractions for flow pattern boundaries (α_1–α_4) are the results from the Schmidt [6] model. The interfacial drag F_i and its coefficients (C_v, C_i) according to the flow regime are listed in Table II. Here, the bubble diameter D_b, the relative velocity V_r and the geometric factor f are defined through Eqs. (5) and (6), where γ is the ratio of bubble diameter D_b and particle diameter d_p.

$$D_b=\min\left(1.35\sqrt{\frac{\sigma}{g(\rho_l-\rho_g)}},\ (\sqrt{2}-1)d_p\right) \tag{5}$$

$$V_r=\frac{V_{sg}}{\alpha}-\frac{V_{sl}}{s},\quad f=\frac{1}{2}(1+\gamma)\ln\left(1+\frac{2}{\gamma}\right) \tag{6}$$

For a smooth transition between flow regimes, the weighting function $W(\xi)$ was adopted as Eq. (7) [5].

$$W(\xi)=\xi^2(3-2\xi)\ \text{where}\ \xi=\frac{\alpha-\alpha_i}{\alpha_{i+1}-\alpha_i} \tag{7}$$

The dimensionless form of Eqs. (1) and (2) can be expressed in as follows:

$$\left(-\frac{dp}{dz}\right)^*=\frac{\rho_l g}{(\rho_l-\rho_g)g}+\frac{F_{pl}^*}{s}-\frac{F_i^*}{s}, \tag{8}$$

$$\left(-\frac{dp}{dz}\right)^*=\frac{\rho_g g}{(\rho_l-\rho_g)g}+\frac{F_{pg}^*}{\alpha}+\frac{F_i^*}{\alpha}, \tag{9}$$

where

$$\left(-\frac{dp}{dz}\right)^*=\frac{-dp/dz}{(\rho_l-\rho_g)g}, \tag{10}$$

$$F^*=\frac{F}{\varepsilon(\rho_l-\rho_g)g}, \tag{11}$$

$$F_{pl}=\varepsilon s\left(\frac{\mu_l}{KK_{rl}}V_{sl}+\frac{\rho_l}{\eta\eta_{rl}}V_{sl}\lvert V_{sl}\rvert\right), \tag{12}$$

$$F_{pg}=\varepsilon\alpha\left(\frac{\mu_g}{KK_{rg}}V_{sg}+\frac{\rho_g}{\eta\eta_{rg}}V_{sg}\lvert V_{sg}\rvert\right). \tag{13}$$

2.2 Dryout Heat Flux

The dryout heat flux, which is the maximum heat flux that can be removed from a unit cross-section of the debris bed, means a coolability limitation for the bed [12]. Thus, the dryout heat flux is one of the most important indicators for evaluating coolability of the debris bed on a reactor containment floor. It can be calculated by solving the mass, momentum, and energy conservation equations. The one-dimensional, time-independent energy conservation equation is expressed as follows:

$$\frac{d}{dz}(\rho_g h_{lg}V_{sg})=Q \tag{14}$$

where h_{lg} is the evaporation latent heat, and Q is the volumetric power density. Thus, the superficial gas velocity is calculated as follows:

$$V_{sg}=\frac{Q\,z}{\rho_g h_{lg}}. \tag{15}$$

The one-dimensional, time-independent mass conservation equation is expressed as follows:

$$\frac{d}{dz}(\rho_g V_{sg}+\rho_l V_{sl})=0 \tag{16}$$

Therefore, the superficial liquid velocity is calculated as follows:

$$V_{sl}=-\frac{\rho_g}{\rho_l}V_{sg}=-\frac{Q\,z}{\rho_l h_{lg}}, \tag{17}$$

and if additional water inflow $V_{sl,0}$ exists from the bottom of bed, it can be expressed as follows:

$$V_{sl}=-\frac{\rho_g}{\rho_l}V_{sg}+V_{sl,0}. \tag{18}$$

The one-dimensional, time-independent momentum conservation equations for liquid and gas are expressed in Eqs. (8) and (9), and the momentum balance equation can be derived by subtracting Eq. (9) from Eq. (8) and multiplying the results by $\alpha(1-\alpha)$. It can be expressed as follows:

$$\alpha(1-\alpha)+\alpha F_{pl}^*-(1-\alpha)F_{pg}^*-F_i^*=0. \tag{19}$$

For the one-dimensional steady-state boiling condition, the heat flux for a void fraction with a range of 0 to 1 can be calculated by solving the Eq. (19). Thus, the dryout heat flux can be obtained with $\alpha=1$ at the top of bed.

3. Preliminary Analysis Cases

To perform preliminary analysis for pressure gradient of two-phase flow and dryout heat flux through beds composed of particles from TROI tests, this study established the analysis cases (TS-VISU and TROI-79–81) [11] among various TROI tests, which exist the available porosity, mass mean diameter data where steam explosion did not occur. The characteristics of analysis cases are illustrated in Figs. 1 and 2. Fig. 1 shows the cumulative mass fraction less than indicated size and Fig. 2 shows the porosity and mass mean diameter for each analysis case.

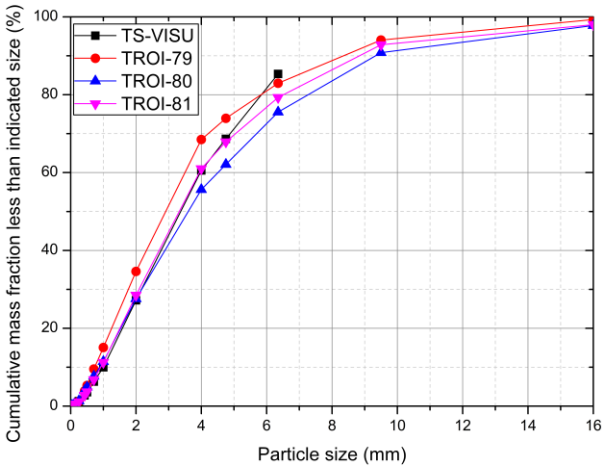

Fig. 1. Cumulative mass fraction less than indicated size [11].

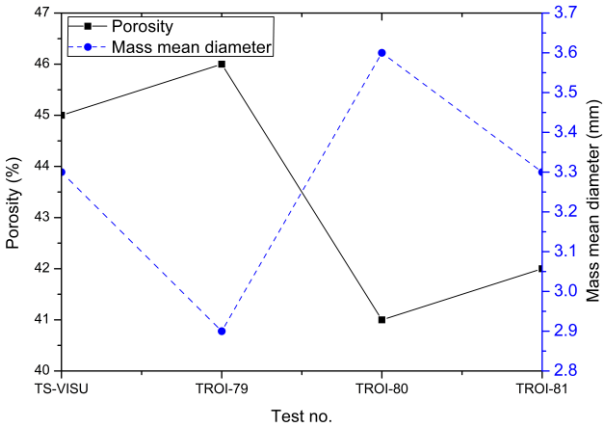

Fig. 2. Porosity and mass mean diameter for test cases [11].

4. Results and Discussions

Fig. 3 illustrates the dimensionless pressure gradients of two-phase flow in beds composed of particles from TROI tests with no additional water inflow under boiling conditions (100°C, 1 bar), which are predicted by existing models with mass mean diameter according to superficial gas velocity (Reed, R [1]; Lipinski, L [2]; Hu and Theofanous, HT [3]; Schulenberg and Müller, SM [4]; Tung and Dhir, TD [5]; Schmidt, S [6]; Rahman, R [7], and Park et al., P [8]). The models are expressed in abbreviation in a legend of Fig. 3.

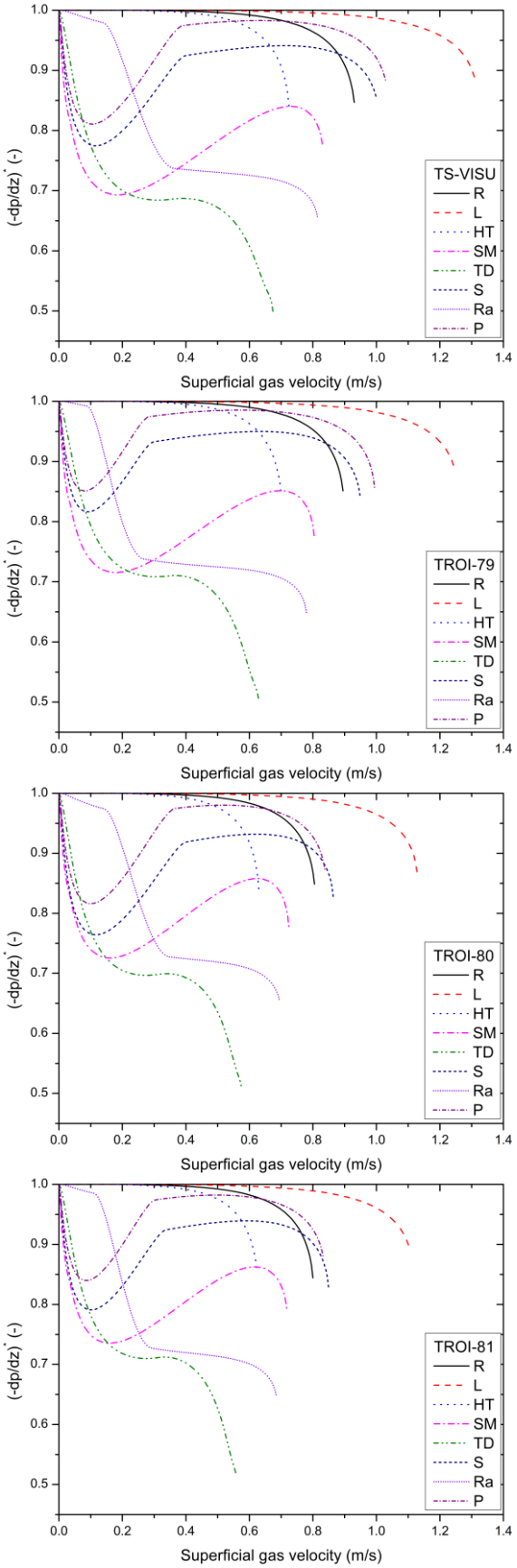

Fig. 3. Dimensionless pressure gradients of two-phase flow in beds with no additional water inflow under boiling conditions, predicted by existing models with mass mean diameter.

The curves illustrate the pressure gradients of two-phase flow in the regime of bubbly, slug, and annular flow as the superficial gas velocity increases. Moreover, the endpoint means the flow limitation point where the calculation ends as the void fraction becomes one. Nevertheless the pressure gradient of two-phase flow is important in a point of view of long-term coolability of ex-vessel debris bed, the predicted pressure gradients and the flow limitation points predicted by numerous models show a significant difference in all cases. The Lipinski model [2] and the Tung and Dhir model [5] predict that the flow limitation occurs at the highest and the lowest superficial gas velocity, respectively.

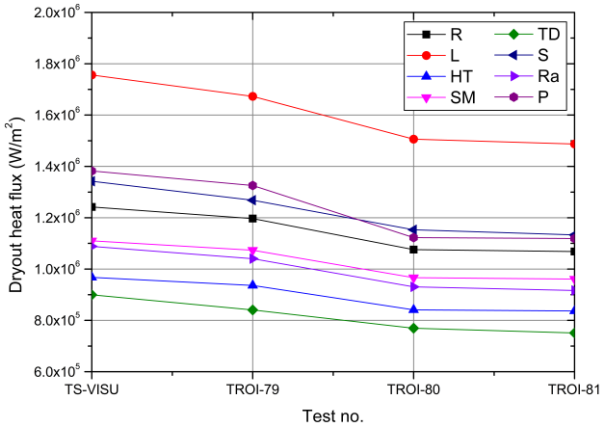

Fig. 4. Dryout heat flux in beds with no additional water inflow, predicted by existing models with mass mean diameter.

Fig. 4 illustrates the dryout heat flux in beds composed of particles from TROI tests with no additional water inflow at 1 bar, which are predicted by existing models with mass mean diameter. The results of dryout heat flux prediction by existing models in all cases illustrate that the highest and lowest values are predicted by the Lipinski model [2] and the Tung and Dhir model [5], respectively. The differences are 195% for TS-VISU, 199% for TROI-79, 196% for TROI-80, and 198% for TROI-81, respectively.

5. Conclusions

The preliminary analysis is performed to investigate the uncertainty of pressure drop and dryout heat flux predicted by the existing two-phase flow models in beds composed of particles from TROI tests (TS-VISU, TROI-79–81) [11], which exist the available porosity, mass mean diameter data where steam explosion did not occur. The analysis results under no additional water inflow at 1 bar describe that the predicted values of pressure gradients and dryout heat flux by numerous models show a significant difference in all cases, indicating that there exists uncertainty for evaluating ex-vessel debris bed coolablity.

Thus, as a further work, experiments (air flow, water/air two-phase flow under atmospheric condition, two-phase flow under boiling condition, and dryout heat flux) are planned to be conducted for evaluating the adequacy of existing models and reducing the uncertainty. Besides, the analysis of the volume and the surface area of particles resulted from TROI test is required to evaluate the adequacy of various mean diameters for non-spherical particles with size distribution (d_{sd} and d_{eq} for non-spherical particle, d_m, d_a, d_l, and d_n for particle size distribution). The experiments using the particles resulted from TROI tests would be extremely meaningful in a point of view of prototypic characteristics.

ACKNOWLEDGMENTS

This work was supported by the National Research Foundation of Korea (NRF) grant funded by the Korea government (Ministry of Science and ICT; Grant No. 2017 M2A8A4015274).

REFERENCES

[1] Reed, A.W., The effect of channeling on the dryout of heated particulate beds immersed in a liquid pool. 1982, Massachusetts Institute of Technology.
[2] Lipinski, R.J., Model for boiling and dryout in particle beds. [LMFBR]. 1982. p. Medium: X; Size: Pages: 177.
[3] Hu, K. and T. Theofanous, On the measurement and mechanism of dryout in volumetrically heated coarse particle beds. International journal of multiphase flow, 1991. 17(4): p. 519-532.
[4] Schulenberg, T. and U. Müller, An improved model for two-phase flow through beds of coarse particles. International journal of multiphase flow, 1987. 13(1): p. 87-97.
[5] Tung, V. and V. Dhir, A hydrodynamic model for two-phase flow through porous media. International journal of multiphase flow, 1988. 14(1): p. 47-65.
[6] Schmidt, W., Influence of multidimensionality and interfacial friction on the coolability of fragmented corium. 2004.
[7] Rahman, S., Coolability of corium debris under severe accident conditions in light water reactors. 2013.
[8] Park, J.H., et al., Modeling of pressure drop in two-phase flow of mono-sized spherical particle beds. International Journal of Heat and Mass Transfer, 2018. 127: p. 986-995.
[9] Park, J.H., et al., Adequacy of effective diameter in predicting pressure gradients of air flow through packed beds with particle size distribution. Annals of Nuclear Energy, 2018. 112: p. 769-778.
[10] Park, J.H., et al., Influence of particle morphology on pressure gradients of single-phase air flow in the mono-size non-spherical particle beds. Annals of Nuclear Energy, 2018. 115: p. 1-8.
[11] Hong, S.-W. and S.M. An, OBSERVATION OF CORIUM DEBRIS CHARACTERISTICS BY FUEL-COOLLANT INTERACTION IN A TROI FACILITY. NTHAS11: The Eleventh Korea-Japan Symposium on Nuclear Thermal Hydraulics and Safety, Busan, Korea, November 18-21, 2018.
[12] Park, J.H., H.S. Park, and M. Lee, A NEW TWO-PHASE PRESSURE DROP MODEL FOR POROUS MEDIA IN BOILING CONDITIONS FOR DRYOUT HEAT FLUX PREDICTION. The 9TH European Review Meeting on Severe Accident Research (ERMSAR2019), Clarion Congress Hotel, Prague, Czech Republic, March 18-20, 2019.